

**SYNTHESIS AND MASS SPECTRAL ANALYSIS OF  
HD DEGRADATION PRODUCTS.  
A COMPUTATIONAL ELUCIDATION OF THE RESULTS.**

Sue Y. Bae, Mark D. Winemiller, Fu-Lian Hsu, Dennis K. Rohrbaugh and  
Harold D. Banks\*

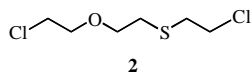
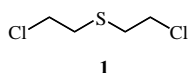
U.S. Army Edgewood Chemical Biological Center, APG, Maryland 21010-5424

**ABSTRACT**

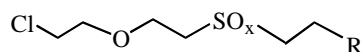
Degradation products that could reasonably form upon storage of sulfur mustard have been synthesized and analyzed by GC/MS. Elucidation of the fragmentation pathways was accomplished by means of B3LYP/6-31+G(d) calculations.

**INTRODUCTION**

Sulfur mustard, HD or bis(2-chloroethyl)sulfide **1** was first introduced as a chemical warfare agent in WW1. Its production has continued to the present, most horrifically against civilians in the 1980's Iran-Iraq war. Due to its ease of synthesis and stockpiling by several countries, its exploitation by terrorists remains an alarming possibility. Numerous publications exist concerning the pathways and products of sulfur mustard degradation under both field and laboratory conditions. One compound, **2**, has been identified spectroscopically in ton containers in quantities approaching 3%; however, direct confirmation



of its presence has not been determined using an authentic synthetic sample. In order to thoroughly study the degradation products of **1**, **2** and ten related sulfides, sulfoxides and sulfones that could reasonably form in the degradation and manufacture of **1** were prepared. These compounds had the following structures:



**2 – 4**, R = CH<sub>2</sub>CH<sub>2</sub>Cl, x = 0 – 2, respectively;  
**5 – 7**, R = CH<sub>2</sub>CH<sub>2</sub>OH, x = 0 – 2, respectively;  
**8 – 10**, R = CH=CH<sub>2</sub>, x = 0 – 2, respectively;

**11** and **12**, x = 0, and R = CH<sub>2</sub>CH<sub>2</sub>OCH<sub>3</sub> and CH<sub>2</sub>CH<sub>2</sub>OCH<sub>2</sub>CH<sub>3</sub>, respectively. Of the arsenal of analytical methods available for characterization of these organosulfur compounds, mass spectrometry (MS) offered the significant advantages of establishing the molecular weights of the compounds (from the molecular ion produced by abstraction of one electron), and in addition, generation of fragmentation patterns that are exquisitely sensitive to specific molecular structure.

While it is possible to intuit fragmentation patterns from available empirical MS data, it is preferable to justify mass spectral assignment in terms of sound theoretical principles. Accordingly, calculations were performed on each mass spectral peak. Transition states for transformation of the fragments were identified in order to estimate the relative intensity of each peak.

Gas chromatography-mass spectrometry was performed on these organosulfur compounds. Analysis was effected both with electron ionization (EI) and collision-induced dissociation (CID) using argon as the neutral gas. The EI mass spectrum typically contains the molecular ion and many fragment ions providing useful structural information. CID is a technique used to confirm the structure of the selected mass ion.

The synthesis of **2** involved the nucleophilic attack of 2-thioethanol on **1** in the presence of NaOCH<sub>3</sub>, followed by conversion of the terminal alcohol functionality into a chloro substituent in 77% overall yield. The remaining potential degradation or side products in the manufacture of **1** involved oxidation chemistry with H<sub>2</sub>O<sub>2</sub>, elimination of HCl using triethylamine, or KOH in methanol or ethanol.

The nature of the mass spectral fragments demands calculations at a reasonably high level that incorporate electron correlation. Considering the computational cost and

anticipated accuracy of the results, density functional theoretical (DFT) methodology was chosen. (Bickelhaupt, 2000; Cramer, 2004) It was decided to use the B3LYP/6-31+G(d) level for which there is considerable literature precedent for calculations in mass spectral elucidation. (Chu, 2008; Baciocchi, 2008; Anand, 2004, Pepe, 1999.)

In summary, eleven compounds relevant to the degradation of **1** upon storage were synthesized and analyzed by gas chromatography/mass spectrometry. The fragmentation patterns were elucidated by means of high level DFT calculations.

## COMPUTATIONAL METHODS

Initial geometries for the ground and transition states for the cations, cation radicals and neutral species were obtained by means of semi-empirical calculations using AM1 methodology. The final DFT calculations were performed by means of the Gaussian suite of programs (Frisch et al., 2004) at the B3LYP/6-31+G(d) level. A scaling factor (Foresman, 1996) of 0.9804 was used for the thermal correction to the computed energies at a temperature of 298.1 K. Criteria for the transition and ground states were calculation of one and zero imaginary frequencies, respectively. Gaussview 3.09 was used to animate the sole imaginary frequency and confirm that the transition state was found on the potential energy surface connecting reactants and products; IRC calculations were used to confirm identification of the transition state. Transition state theory was employed in calculation of the free energies of activation. (Lowry, 1981.)

## GAS CHROMATOGRAPHY-MASS SPECTROMETRY

An Agilent 5975 mass spectrometer interfaced to an Agilent 6890 gas chromatograph was used for gas chromatographic-mass spectral analysis. An Agilent J&W Scientific HP-5ms bonded phase capillary column (30 m x 0.25 mm i.d.) with a film thickness of 0.25  $\mu\text{m}$ . The injection port temperature was 220  $^{\circ}\text{C}$ , the GC-MS interface temperature was 250  $^{\circ}\text{C}$  and the source temperature was 150  $^{\circ}\text{C}$ . The carrier gas was helium with a flow rate of 1 mL/min and the oven temperature was programmed from 60 to 250  $^{\circ}\text{C}$  at 15  $^{\circ}\text{C}/\text{min}$ . A split injector was used (split ratio 75:1) and 0.2  $\mu\text{L}$  volume

of sample was placed on the column. The mass range scanned was from 50 to 450 Da at 4 scans per second.

The gas chromatography-tandem mass spectrometry (GC-MS-MS) analysis was performed on a Finnigan TSQ-7000 GC-MS-MS (San Jose, CA, U.S.) interfaced to a Varian 3400 gas chromatograph (Palo Alto, CA, U.S.). The instrument was equipped with a 30 m x 0.25 mm i.d. HP-5ms capillary column with a film thickness of 0.25  $\mu\text{m}$ . The injector port temperature was 250  $^{\circ}\text{C}$ , the GC-MS interface temperature was 250  $^{\circ}\text{C}$  and the source temperature was 150  $^{\circ}\text{C}$ . The carrier gas was helium with a flow rate of 1 mL/min and the oven temperature was programmed from 60 to 250  $^{\circ}\text{C}$  at 15  $^{\circ}\text{C}/\text{min}$ . A split injector was used (split ratio 75:1) and 0.5  $\mu\text{L}$  volume of sample was placed on the column manually. Argon was used as the collision gas for the CID. The pressure in the collision cell was 1.5 mT and the collision energy was -15 eV. The mass range scanned was from 20 to 200 Da at 1 scan/s. Qualitative and quantitative analyses were processed by Xcalibur<sup>TM</sup> (Finnigan MAT, San Jose, CA, U.S.) software supplied with the MS data system. The mass ion of interest was selected for each individual compound and the retention time, peak area and relative percent abundance of the fragment ions were calculated (Table 1).

## SYNTHETIC PROCEDURES

The compounds studied herein were prepared by previously reported procedures (Winemiller, 2008.) As an example, the preparation of **2** was accomplished by the nucleophilic displacement of chloride from bis(2-chloroethyl)ether by 2-thioethanol in the presence of NaOMe followed by chlorination of the product with  $\text{SOCl}_2$ .

## MASS SPECTROMETRIC RESULTS

**2:** The EI mass spectrum exhibits the molecular ion at  $m/z$  202 and isotopic ions at  $m/z$  204 and  $m/z$  206 due to chlorine. Higher mass ions due to  $[\text{M}-\text{HCl}]^+$ ,  $[\text{M}-\text{OCH}_2\text{CH}_2\text{Cl}]^+$  and  $[\text{M}-\text{CH}_2\text{SCH}_2\text{CH}_2\text{Cl}]^+$  are observed at  $m/z$  166,  $m/z$  123 and  $m/z$  93. The mass ion at  $m/z$  123 was selected for CID and produced three major product ions at  $m/z$  63,  $m/z$  87 and  $m/z$  95 due to  $[\text{C}_2\text{H}_4\text{Cl}]^+$ ,  $[\text{C}_4\text{H}_7\text{S}]^+$  and  $[\text{C}_2\text{H}_4\text{SCl}]^+$  respectively, with a relative intensity ratio of 100:1:13.

**3:** The EI mass spectrum shows three principal ions with  $m/z$  values of 63, 76 and 107. The higher mass ion at  $m/z$  107 was formed due to  $[M-C_2H_4OSCl]^+$  and the lower mass ion at  $m/z$  63 was from loss of  $C_4H_8SO_2Cl$ . The mass ion at  $m/z$  107 was selected for CID and produced two major product ions with  $m/z$  63,  $[ClCH_2CH_2]^+$  and  $m/z$  45,  $[C_2H_5O]^+$  with a relative intensity ratio of 100:12.

**4:** The EI mass spectrum shows five principal ions with  $m/z$  values of 63, 106, 127, 155 and 185. The higher mass ions at  $m/z$  155 and  $m/z$  185 were formed due to  $[M-C_2H_5OCl]^+$  and  $[M-CH_2Cl]^+$ . Two higher mass EI fragmentation ions ( $m/z$  155 and  $m/z$  185) were selected for CID. Three product ions at  $m/z$  63,  $m/z$  93 and  $m/z$  127 due to  $[ClCH_2CH_2]^+$ ,  $[C_2H_5SO_2]^+$  and  $[C_2H_4SO_2Cl]^+$  respectively with a relative intensity ratio of 100:8:24, were observed in the CID spectrum of  $m/z$  155. The CID of  $m/z$  185 contains three major product ions with  $m/z$  values of 63 (loss of  $C_3H_6SO_3$ ), 127 (loss of  $C_3H_6O$ ) and 155 (loss of  $CH_2O$ ), with a relative intensity ratio of 25:26:100.

**5:** The EI mass spectrum exhibits a molecular ion at  $m/z$  184 and an isotopic ion at  $m/z$  186 due to chlorine. Higher mass ions due to  $[M-HCl]^+$ ,  $[M-OCH_2CH_2Cl]^+$ , and  $[M-OC_3H_6Cl]^+$  are observed at  $m/z$  148,  $m/z$  105 and  $m/z$  91 respectively. The mass ion at  $m/z$  105 was selected for CID and produced three major product ions with  $m/z$  values of 87, 61 and 45 with a relative intensity ratio of 13:42:100. The  $m/z$  87 was due to loss of  $H_2O$ , the  $m/z$  61 was due to loss of  $C_2H_4O$  and the  $m/z$  45 was due to loss of  $CH_2CH_2S$ .

**6:** The EI mass spectrum contains the molecular ion at  $m/z$  200 and an isotopic ion at  $m/z$  202 due to chlorine. Higher mass ions due to  $[M-HCl]^+$ ,  $[M-C_2H_5SO_2]^+$  and  $[M-OC_5H_9Cl]^+$  are observed at  $m/z$  165,  $m/z$  107 and  $m/z$  94 respectively. The lower mass ion at  $m/z$  63 was due to loss of  $C_4H_9SO_3$ . The mass ion at  $m/z$  107 was selected for CID and produced two major product ions at  $m/z$  63 and  $m/z$  45, due to  $[C_2H_4Cl]^+$  and  $[C_2H_5O]^+$  respectively with a relative intensity ratio of 100:12.

**7:** The EI mass spectrum shows six principal ions with  $m/z$  values of 167, 137, 109, 93, 79 and 63. The higher mass ions at  $m/z$  167 and  $m/z$  109 were formed due to  $[M-CH_2Cl]^+$  and  $[M-CH_2CH_2OCH_2CH_2Cl]^+$ . Two EI fragments ( $m/z$  137 and  $m/z$  167) were selected for CID. Three

product ions at  $m/z$  93,  $m/z$  109 and  $m/z$  119 due to  $[C_4H_7SO_2]^+$ ,  $[C_2H_5SO_3]^+$  and  $[C_2H_5SO_2]^+$  respectively with a relative intensity ratio of 8:40:1, were observed in the CID spectrum of  $m/z$  137. The CID of  $m/z$  167 contains three major product ions with  $m/z$  values of 45 (loss of  $C_3H_6SO_3$ ), 109 (loss of  $C_3H_6O$ ) and 137 (loss of  $HCHO$ ), with a relative intensity ratio of 15:34:100.

**8:** The EI mass spectrum contains the molecular ion at  $m/z$  166 and isotopic ions at  $m/z$  168 and  $m/z$  170 due to chlorine. Higher mass ions at  $m/z$  131 and  $m/z$  106 were formed due to  $[M-Cl]^+$  and  $[M-C_3H_4S]^+$ . Three potential resonance structures exist from the loss of Cl from the molecular ion. The lower mass ions at  $m/z$  63 (loss of  $C_4H_7SO$ ) and  $m/z$  43 (loss of  $CH_2CH_2Cl$ ) are shown in Figure 8b. The CID of the mass ion at  $m/z$  166 depicts three product ions with  $m/z$  values of 43, 63 and 131 with a relative intensity ratio of 68:29:3.

**9:** The EI mass spectrum of **8** contains the molecular ion at  $m/z$  182 and a higher mass ion due to  $[M-C_4H_8OCl]^+$  at  $m/z$  107. The CID of  $m/z$  107 contains two major product ions at  $m/z$  45 and  $m/z$  63 due to  $[C_2H_5O]^+$  and  $[CH_2CH_2Cl]^+$  respectively, with a relative intensity ratio of 12:100.

**10:** The EI mass spectrum shows four principal ions with  $m/z$  values of 63, 91, 106 and 149. Higher mass ions at  $m/z$  149 and  $m/z$  106 were formed due to  $[M-CH_2Cl]^+$  and  $[M-C_2H_4SO_2]^+$ . Lower mass ions at  $m/z$  63 and  $m/z$  91 were formed due to  $[M-C_4H_7SO_3]^+$  and  $[M-C_4H_8OCl]^+$  (Figure 10a). The CID of  $m/z$  149 contains two major product ions at  $m/z$  91 and  $m/z$  119 due to  $[C_2H_5SO_2]^+$  and  $[C_4H_7SO_2]^+$  respectively, with a relative intensity ratio of 100:99.

**11:** The EI mass spectrum contains the molecular ion at  $m/z$  198. The higher mass ion at  $m/z$  119 was formed due to  $[M-OCH_2CH_2Cl]^+$ . Lower mass ions at  $m/z$  103 and  $m/z$  59 were formed due to  $[M-OCH_3-ClCH_2]^+$  and  $[M-C_3H_8O-OCH_2CH_2Cl]^+$ . The CID of  $m/z$  119 contains two major product ions at  $m/z$  59 and  $m/z$  87 due to  $[C_2H_3S]^+$  and  $[C_4H_7S]^+$  respectively, with a relative intensity ratio of 100:11.

**12:** The EI mass spectrum shows molecular ion at  $m/z$  212. The higher mass ion at  $m/z$  177 was formed due to  $[M-Cl]^+$  forming one of three

resonance structures. Another higher mass ion at  $m/z$  133 formed due to  $[M - OCH_2CH_2Cl]^+$  could be from one of two resonance structures. The CID of  $m/z$  133 contains four major products  $m/z$  45,  $m/z$  73,  $m/z$  87 and  $m/z$  105 due to  $[C_2H_5O]^+$ ,

$[C_4H_9O]^+$ ,  $[C_4H_7S]^+$ , and  $[C_4H_9SO]^+$  respectively, with a relative intensity ratio of 98:100:7:6.

$[C_2H_3SO_2]^+$  and  $[C_4H_7SO_2]^+$  respectively, with a relative intensity ratio of 100:99.

## RESULTS AND DISCUSSION

Since **2** has been found in measurable quantities in mustard storage containers, it was decided to initially focus on the analysis of this compound to define the parameters for the remaining compounds in the series.

The EI mass spectrum of **2** contains the molecular ion at  $m/z$  202 and  $m/z$  166, 123 and 93. When mass ion  $m/z$  123 was selected for CID three major product ions were produced at  $m/z$  63,  $m/z$  87 and  $m/z$  95. The full proposed fragmentation pathway is illustrated in Scheme 1.

In order to verify this scheme, DFT calculations were performed on the molecular ion, and also on each of the fragments. In addition, the free energies of activation of the transition states were calculated to assess the plausibility of the intensity of the fragment ions. The results of this calculation are provided in Table 1. In order to determine the appropriateness of the level of the calculations, a higher order basis set, 6-311+G(d) was used for Reaction C and the result compared to that obtained using our standard basis set. Higher-order basis sets demand considerably

**SCHEME 1**

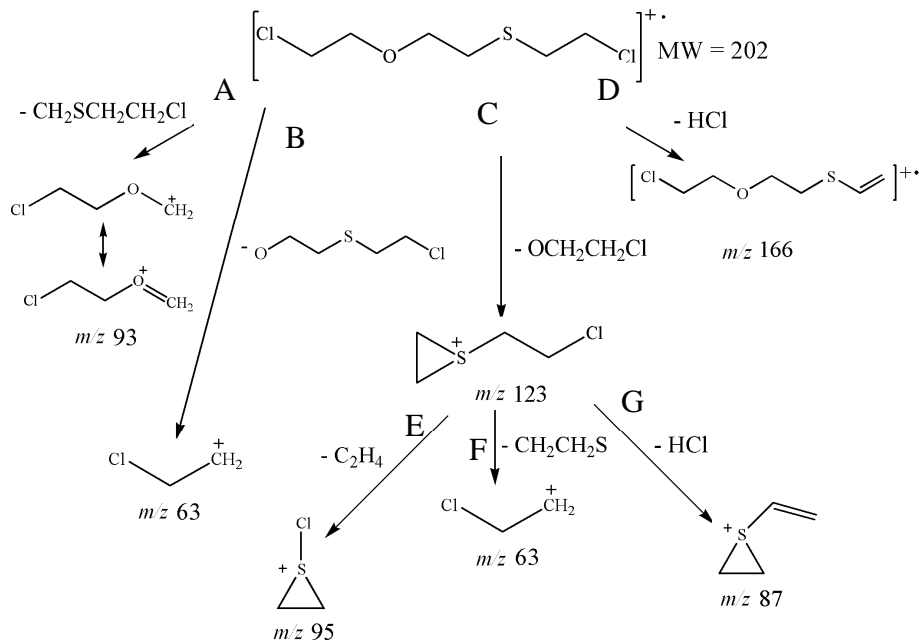


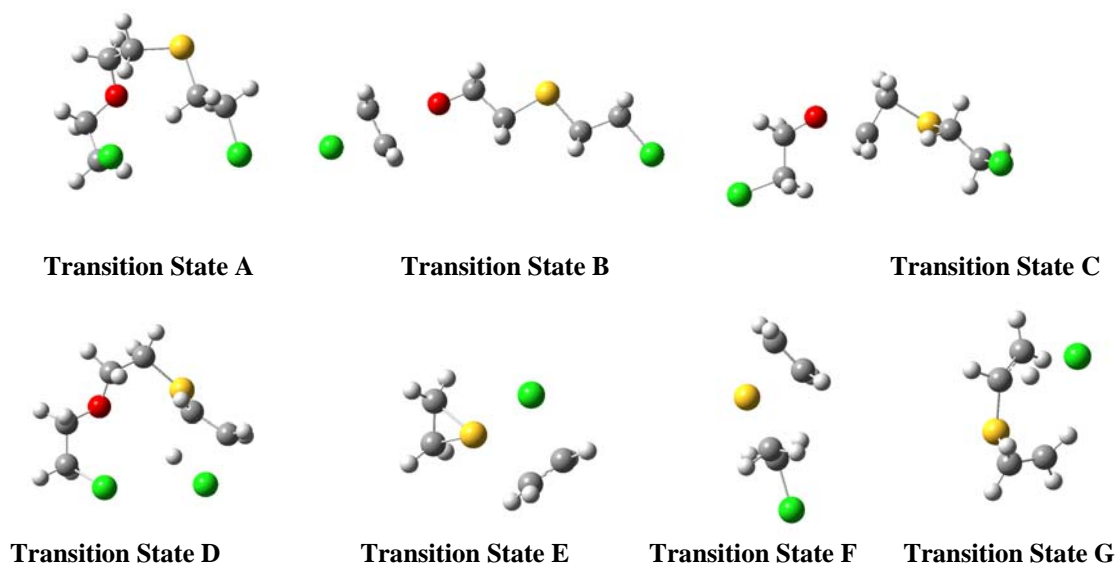
**TABLE 1**

Reaction (see chart)	$[E_{\text{corr}}]_{\text{GS}}$ hartrees	$[E_{\text{corr}}]_{\text{TS}}$ hartrees	$\Delta E^\ddagger$ kcal/mol	$\Delta H^\ddagger$ kcal/mol	$S_{\text{GS}}$ eu	$S_{\text{TS}}$ eu	$\Delta S^\ddagger$ eu	$\Delta G^\ddagger$ kcal/mol	$\Delta G^\ddagger$ kJ/mol	$\Delta G^\ddagger$ eV
<b>A</b>	-1629.175406	-1629.175590	-0.115	0.478	126.64	117.20	-9.433	3.29	13.8	0.14
<b>B</b>	-1629.175406	-1629.094208	50.95	51.55	126.64	124.73	-1.905	52.1	218.0	2.26
<b>C</b>	-1629.175406	-1629.118185	35.91	36.50	126.64	127.85	1.216	36.1	151.2	1.57
<b>D</b>	-1629.175406	-1629.113152	39.07	39.66	126.64	119.16	-7.476	41.9	175.3	1.82
<b>E</b>	-1015.216590	-1015.098082	74.36	74.96	87.382	90.713	3.331	74.0	309.5	3.21
<b>F</b>	-1015.216590	-1015.160039	35.49	36.08	87.382	88.052	0.67	35.9	150.1	1.56
<b>G</b>	-1015.216590	-1015.126255	56.69	57.28	87.382	87.184	-0.198	57.3	239.9	2.49
<b>C [6-311++G(d)]</b>	-1629.342507	-1629.282150	37.87	38.47	126.64	127.85	1.215	38.1	159.4	1.65

Higher-order basis increased computational time.  
The free energies of activation were only

different by 2.0 kcal/mol providing support for  
our computational methodology.

**FIGURE 1. TRANSITION STATES LEADING TO THE FRAGMENTATION PATTERN MOLECULAR ION OF 2.**



State-of-the art calculations using this methodology are unable to predict intensities of the fragment ions in the mass spectrum. Obtaining plausible energies and structures for the stable ions and the transition states leading to them provides strong support for the Scheme 1.

Table 2 provides the energies of the fragment ions, their entropies and illustrates that all calculated frequencies are positive by giving the value of the lowest calculated vibrational frequency.

**TABLE 2**

	Energy hartrees	Therm. Corr. hartrees	Corr. Energy hartrees	Entropy eu	Lowest Frequency
<i>mz 87</i>	-554.5110071	0.1053210	-554.4077504	77.7	51.6
<i>mz 95</i>	-936.6790049	0.0621410	-936.6180819	71.4	225.0
<i>mz 123</i>	-1015.3364636	0.1222700	-1015.2165901	87.4	58.3
<i>mz 166</i>	-1168.5456462	0.1742400	-1168.3748213	113.7	25.8
<i>MZ 93</i>	-653.0224172	0.0949950	-652.9292841	79.1	79.1
<i>MZ 63</i>	-538.4656706	0.0592530	-538.4075790	63.0	476.2
<b>MW202</b>	-1629.3619685	0.1902920	-1629.1754062	126.6	11.5
<b>HCl</b>	-460.7979997	0.0090240	-460.7891526	44.6	2925.1
<b>thiirane</b>	-476.7874231	0.0586370	-476.7299354	62.3	629.4
<b>CH<sub>2</sub>SCH<sub>2</sub>CH<sub>2</sub>Cl</b>	-976.2670189	0.0895060	-976.1792672	85.5	56.4
<b>CH<sub>2</sub>=CH<sub>2</sub></b>	-78.5932689	0.0541440	-78.5401861	53.7	837.1
<b>OCH<sub>2</sub>CH<sub>2</sub>Cl</b>	-613.9696705	0.0691350	-613.9018905	71.9	130.9
<b>OCH<sub>2</sub>CH<sub>2</sub>SCH<sub>2</sub>CH<sub>2</sub>Cl</b>	-1090.7882904	0.1248430	-1090.6658943	100.7	33.6

## CONCLUSIONS

DFT calculations using the 6-31G +(d) basis set have been applied to the elucidation of the EI and CID spectra of **2**, found in HD storage containers. A computation using a higher, more expensive basis produced only minor changes in the energy calculations. While computational reproduction of spectral intensities is beyond the capability of the method employed, the calculations were able to establish the relative energies of the radical and the cationic and radical products, and establish that the reactants and products could be connected by means of a reasonable transition state. Our conclusions for additional members of this series of compounds have been similar to those for **2**.

## REFERENCES

- Anand, S.; Zamari, M.M.; Menkir, G.; Levis, R.J.; Schlegel, H.B. *J. Phys. Chem A*, **2004**, *108*, 3162 – 3165.
- Baciacchi, E.; Del Giacco, T.; Lanzalunga, O.; Mencarelli, P.; Procacci, B. *J. Org. Chem.* **2008**, *73*, 5675 – 5682.
- Bickelhaupt, M.F.; Baerends, J.E. in *Reviews in Computational Chemistry*, 15, Lipowitz, K.B.; Boyd, D.B. Eds., Wiley-VCH: New York, 2000, pp 1 – 87.
- Chu, I.K.; Zhao, J.; Xu, M.; Siu, S.O.; Hopkinson, A.C.; Siu, K.W.M., *J. Am. Chem. Soc.* **2008**, *130*, 7862 – 7872.
- Cramer, C. J. *Essentials of Computational Chemistry*, 2<sup>nd</sup> Ed., Wiley: New York, 2004, p. 249 – 303.
- Foresman, J.B., Frisch, A. *Exploring Chemistry with Electronic Structure Methods*, 2<sup>nd</sup> Ed., Gaussian, Inc.: Pittsburgh, PA, 1996.
- Friesner, R.A. *PNAS*, **2005**, *102*, 6648 – 6653.
- Frisch, M. J.; Trucks, G. W.; Schlegel, H. B.; Scuseria, G. E.; Robb, M. A.; Cheeseman, J. R.; Montgomery, Jr., J. A.; Vreven, T.; Kudin, K. N.; Burant, J. C.; Millam, J. M.; Iyengar, S. S.; Tomasi, J.; Barone, V.; Mennucci, B.; Cossi, M.; Scalmani, G.; Rega, N.; Petersson, G. A.; Nakatsuji, H.; Hada, M.; Ehara, M.; Toyota, K.; Fukuda, R.; Hasegawa, J.; Ishida, M.; Nakajima, T.; Honda, Y.; Kitao, O.; Nakai, H.; Klene, M.; Li, X.; Knox, J. E.; Hratchian, H. P.; Cross, J. B.; Bakken, V.; Adamo, C.; Jaramillo, J.; Gomperts, R.; Stratmann, R. E.; Yazyev, O.; Austin, A. J.; Cammi, R.; Pomelli, C.; Ochterski, J. W.; Ayala, P. Y.; Morokuma, K.; Voth, G. A.; Salvador, P.; Dannenberg, J. J.; Zakrzewski, V. G.; Dapprich, S.; Daniels, A. D.; Strain, M. C.; Farkas, O.; Malick, D. K.; Rabuck, A. D.; Raghavachari, K.; Foresman, J. B.; Ortiz, J. V.; Cui, Q.; Baboul, A. G.; Clifford, S.; Cioslowski, J.; Stefanov, B. B.; Liu, G.; Liashenko, A.; Piskorz, P.; Komaromi, I.; Martin, R. L.; Fox, D. J.; Keith, T.; Al-Laham, M. A.; Peng, C. Y.; Nanayakkara, A.; Challacombe, M.; Gill, P. M. W.; Johnson, B.; Chen, W.; Wong, M. W.; Gonzalez, C.; and Pople, J. A.; Gaussian, Inc., Wallingford CT, 2004. [Gaussian 03, Revision C.02]
- Lowry, T.H.; Richardson, K.S. *Mechanism and Theory in Organic Chemistry*, 2<sup>nd</sup> Ed., Harper & Row: New York, 1981, p 194.
- Winemiller, M.D. and Sumpter, K.B., 2008: Products of Sulfur Mustard Degradation: Synthesis and Characterization of 1-(2-chloroethoxy)-2-[(2-chloroethyl)thio]ethane, Related Compounds and Derivatives, *Phosphorus, Sulfur and Silicon and the Related Elements*, in press.